The Temperature Diffuse Scattering of X-Rays by Potassium Chloride and Potassium Bromide Crystals

JANE HAMILTON HALL*
Ryerson Physical Laboratory, The University of Chicago, Chicago, Illinois
(Received September 22, 1941)

The temperature diffuse scattering of x-rays by KCl and KBr crystals has been investigated with Cu $K\alpha$ radiation. The displacements of the temperature diffuse maxima from the Bragg scattering angle have been obtained experimentally for various settings of the crystal near the 400, 420 and 440 Bragg reflections. The theoretical displacement curve for the special case of KCl has been accurately calculated by considering the relative effects of the α_1 and α_2 wavelengths at the different angles of incidence used. The experimental results are found to be in good agreement with the theory when this is done. The half-widths and relative intensities have been noted experimentally and suitable corrections applied for the vertical divergence of the slit system. An attempt has been made to determine the elastic constants of KBr from diffuse scattering data.

INTRODUCTION

THE present existence of three widely differing theories[1–6] concerning the diffuse scattering of x-rays has led to many experimental studies of this phenomena. Three recent papers in particular have appeared which made it desirable to carry out further investigations in greater detail. The first of these papers[5] treated very rigorously the theory of the temperature diffuse scattering of x-rays and led to results which had been found previously by experimental workers. The second of these articles[7] reported that the observed displacements of the diffuse maxima from the Bragg scattering angle did not agree with the temperature diffuse theory. These displacements had been calculated, however, from an approximate formula to be found in an earlier publication.[8] Re-calculation of the published data by the more rigorous formula appearing in the theoretical paper mentioned above resulted in excellent agreement with the theory.[9] These data were for sodium chloride. The third paper[10] mentioned above reported an agreement in the half-widths calculated and observed for potassium chloride. The half-widths in this case had been calculated by the approximate formula. The more exact theory predicts considerably smaller half-widths. It was therefore decided to carry out further work on potassium chloride to check the half-widths of the diffuse maxima and to measure the displacements of these maxima from the Bragg angle of scattering. Potassium chloride is a convenient substance to use because it may be treated as a simple cubic crystal and because the elastic constants which enter directly into the theory are well known from other sources. If it is assumed that the Cauchy relation is satisfied for KBr, the ratio of the elastic constants should be obtainable from diffuse scattering data. An attempt was made to determine these constants. The only partial success will be discussed in a latter section of the paper.

THE THEORY OF THE TEMPERATURE DIFFUSE SCATTERING OF X-RAYS

The x-radiation scattered by a normal crystal may be divided into three components. The first (and coherent) part is the Laue-Bragg scattering which exhibits sharp maxima in the Laue directions and is zero elsewhere. The incoherent part consists of the Compton diffuse scattering and the temperature diffuse scattering. From

* Now at the University of Denver.
[1] C. V. Raman and P. Nilakantan, Proc. Indian Acad. Sci. **11**, 379, 389, 398 (1940); Nature **147**, 805 (1941); Phys. Rev. **60**, 63 (1941); Current Science **5**, 241 (1941).
[2] W. H. Bragg, Nature **146**, 509 (1940); **148**, 112 (1941).
[3] G. D. Preston, Nature **143**, 76 (1939); **147**, 358 (1941); **147**, 467 (1941).
[4] M. Born, Nature **147**, 674 (1941).
[5] W. H. Zachariasen, Phys. Rev. **59**, 860 (1941).
[6] M. Born and K. Sarginson, Proc. Roy. Soc. **179**, 69 (1941).
[7] G. E. M. Jauncey and O. J. Baltzer, Phys. Rev. **59**, 699 (1941).
[8] W. H. Zachariasen, Phys. Rev. **57**, 597 (1940).
[9] W. H. Zachariasen, Phys. Rev. **59**, 909 (1941).
[10] S. Siegel, Phys. Rev. **59**, 371 (1941).

considerations of the equilibrium positions of the atoms in a simple cubic lattice and of the vibrations of the atoms in this lattice it has been shown[5] that the temperature diffuse scattering intensity may be written as

$$J=\frac{NI_a}{4\pi^2 m_a \tau_0^2}\sum_j \frac{(\boldsymbol{s}\cdot\boldsymbol{A}_j)^2}{v_j^2}Q_j, \tag{1}$$

where $\boldsymbol{\tau}_0=\boldsymbol{B}_H-\boldsymbol{k}-\boldsymbol{k}_0$ and is the wave vector of a vibrational mode of the lattice, I_a is the intensity of coherent scattering from one atom, N is the number of atoms, m_a is the atomic mass, $\boldsymbol{k}_0$ is the incident wave vector, $\boldsymbol{k}$ is the scattered wave vector, $\boldsymbol{B}_H$ a reciprocal lattice vector, $\boldsymbol{s}=2\pi(\boldsymbol{k}-\boldsymbol{k}_0)$, A_j is the jth polarization direction associated with the wave vector $\boldsymbol{\tau}_0$, v_j the propagation velocity corresponding to the jth polarization direction.

$$Q_j=\frac{h\nu_j}{\exp(h\nu_j/kT)-1}+\frac{h\nu_j}{2}.$$

It has been shown[5,11,12] that the equations of motion of a simple cubic lattice which consider only the atomic interaction between nearest and next nearest neighbors may be written as a set of linear homogeneous equations from which the frequency and polarization direction may be obtained. The equations may be written as:

$$[\boldsymbol{\phi}(\tau)-v^2\mathbf{1}]\cdot\boldsymbol{A}=0, \tag{2}$$

where $\mathbf{1}$ is the unit tensor and $\boldsymbol{\phi}$ a symmetrical tensor. In the Cartesian system which has its coordinate axes along the cube edges,

$$\phi_{11}=\frac{a+2b-[a+b(\cos 2\pi\tau_2+\cos 2\pi\tau_3)]\cos 2\pi\tau_1}{\tau^2},$$

$$\phi_{12}=\frac{b\sin 2\pi\tau_1 \sin 2\pi\tau_2}{\tau^2}.$$

τ_1, τ_2, τ_3 are components of τ in the reciprocal lattice.

$$a=\alpha/2\pi^2 m_a, \quad b=\gamma/\pi^2 m_a.$$

α and γ are the force constants for nearest and next nearest neighbors and are equal to[11]

$$\alpha=a_0(c_{11}-c_{12}-c_{44}),$$

$$4\gamma=a_0(c_{12}+c_{44}),$$

where a_0 is the edge of the unit cell. It is seen that the three real roots of the secular equation

$$|\boldsymbol{\phi}-v^2\mathbf{1}|=0$$

will be the propagation velocities v_j^2. Furthermore, if the vibrational wave number is small so that $\sin 2\pi i=2\pi i$, the tensor may be expanded to

$$\boldsymbol{\phi}=2\pi^2 a_0^2 b[\mathbf{1}+2\boldsymbol{nn}]+2\pi^2 a_0^2(a-b)\begin{bmatrix}\alpha_1^2 & 0 & 0\\ 0 & \alpha_2^2 & 0\\ 0 & 0 & \alpha_3^2\end{bmatrix}. \tag{3}$$

Here $\boldsymbol{\tau}=\tau\boldsymbol{n}$ and α_1, α_2, α_3 are the direction cosines of $\boldsymbol{n}$ relative to the cube edges, $\boldsymbol{n}$ being the unit vector along the propagation direction.

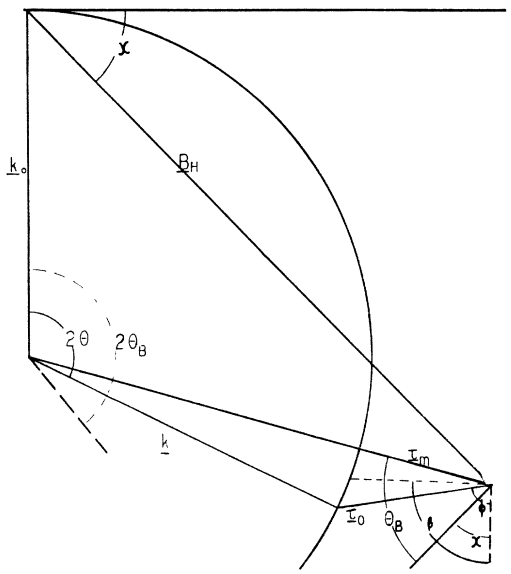

FIG. 1. A section of the reciprocal lattice drawn for an *HKO* reflection, Δ being negative.

Before developing the general theory further it will be convenient to discuss Fig. 1 which shows the reciprocal lattice construction for the scattering process. It will be valuable in geometrically interpreting the equations to follow.

[11] M. Born and Th. v. Kármán, Physik. Zeits. **13**, 297 (1912).
[12] M. Blackman, Proc. Roy. Soc. **148**, 365, 384, (1935); **159** 416 (1937).

The general case is drawn in which the plane of reflection does not lie along a cube face as in the case of an *HOO* reflection but is at an angle with the cube face. This will correspond to an *HKO* reflection. 2θ is the scattering angle for the diffuse radiation; $2\theta_B$ is the Bragg scattering angle; and $\boldsymbol{B}_H$ is a reciprocal lattice vector corresponding to an *HKO* plane. $\boldsymbol{k}_0$ is the wave vector of the incident x-rays, while $\boldsymbol{k}$ is the wave vector of the scattered x-rays. $\boldsymbol{\tau}_0$ is the wave vector of an elastic wave and is given by the relation $\boldsymbol{k}-\boldsymbol{k}_0+\boldsymbol{\tau}_0=\boldsymbol{B}_H$. τ_m is the minimum value which $\boldsymbol{\tau}_0$ will assume as $\boldsymbol{k}$ varies. θ_B is in reality $\theta_B-\Delta\cos 2\theta_B$ ($\theta_B-\Delta$) is the actual glancing angle of incidence) but the second term may be neglected when Δ is small. The angle ϕ is the angle between the cube edge and the varying $\boldsymbol{\tau}_0$. For each plane of reflection there will be a different value of ϕ for which the intensity of scattering is a maximum. The dotted line shown is the direction of polarization of the quasi-longitudinal wave which makes an angle β with the wave vector. In general, none of the three polarization directions will coincide with the propagation directions. This means that none of the three waves is purely longitudinal or purely transverse.

Returning now to the intensity expression of Eq. (1) and the tensor $\boldsymbol{\phi}$ [Eq. (3)] it is seen that the first term of $\boldsymbol{\phi}$ is a tensor with rotational symmetry about the propagation direction $\boldsymbol{n}$. (It has been stated that $\boldsymbol{\tau}=\tau\boldsymbol{n}$.) If in Eq. (3) $c_{11}=3c_{12}$ the second term becomes zero and the three waves resulting will be one longitudinal and two transverse. This is a special case but is rather closely approximated by sodium chloride.

The most general case of a cubic crystal for which the Cauchy relation holds will be treated in the following discussion. Not all crystals showing cubic symmetry will fulfill the Cauchy relation which demands that the elastic constant c_{12} equal the constant c_{44}.[6] For the alkali halides at room temperature the condition is, in general, satisfied. The elastic constants for KCl have the values[7] $c_{11}=3.76\times10^{11}$ dynes/cm^2; $c_{12}=0.64\times10^{11}$ dynes/cm^2; $c_{44}=0.63\times10^{11}$ dynes/cm.[2] When the tensor $\boldsymbol{\phi}$ is expanded the result

$$\boldsymbol{\phi}=\frac{c_{12}V}{m_a}\begin{pmatrix}1+2\alpha_1^2 & 2\alpha_1\alpha_2 & 2\alpha_1\alpha_3\\ 2\alpha_2\alpha_1 & 1+2\alpha_2^2 & 2\alpha_2\alpha_3\\ 2\alpha_3\alpha_1 & 2\alpha_3\alpha_2 & 1+2\alpha_3^2\end{pmatrix}+(c_{11}-3c_{12})\frac{V}{m_a}\begin{pmatrix}\alpha_1^2 & 0 & 0\\ 0 & \alpha_2^2 & 0\\ 0 & 0 & \alpha_3^2\end{pmatrix} \quad (4)$$

is obtained. If K is allowed to equal c_{11}/c_{12}

$$\boldsymbol{\phi}=\frac{c_{12}V}{m_a}\begin{pmatrix}1+(K-1)\alpha_1^2 & 2\alpha_1\alpha_2 & 2\alpha_1\alpha_3\\ 2\alpha_2\alpha_1 & 1+(K-1)\alpha_2^2 & 2\alpha_2\alpha_3\\ 2\alpha_3\alpha_1 & 2\alpha_3\alpha_2 & 1+(K-1)\alpha_3^2\end{pmatrix}.$$

If $\boldsymbol{k}_0$ and $\boldsymbol{k}$ lie in a cube face and if $\boldsymbol{B}_H$ is of the type $\boldsymbol{B}_{H_1H_2O}$, it follows that $\alpha_3=0$. When one sets $\alpha_3=0$ and substitutes for α_1 and α_2 the values of the sin or cos function of the angle ϕ (Fig. 1) he finds that the tensor reduces immediately to one of second order of the form

$$\boldsymbol{\phi}=\frac{c_{12}V}{m_a}\begin{pmatrix}1+(K-1)\cos^2\phi & 2\cos\phi\sin\phi & 0\\ 2\cos\phi\sin\phi & 1+(K-1)\sin^2\phi & 0\\ 0 & 0 & 1\end{pmatrix}.$$

Hence, $v_3^2=c_{12}V/m_a$ while $\boldsymbol{A}_3$ becomes the third Cartesian coordinate vector $\boldsymbol{k}$. From Eq. (2) two linear homogeneous equations are obtained by substituting the expression for $\boldsymbol{\phi}$. Here $\boldsymbol{A}$ is equal to $\boldsymbol{A}_x\boldsymbol{i}+\boldsymbol{A}_y\boldsymbol{j}+\boldsymbol{A}_z\boldsymbol{k}$ and v^2 is set equal to $(V/m_a)c_{12}x$

$$(1+\cos^2\phi(K-1)-x)A_x+(2\cos\phi\sin\phi)A_y=0.$$

$$(2\cos\phi\sin\phi)A_x+(1+(K-1)\sin^2\phi-x)A_y=0.$$

Solving these for x results in

$$x=\frac{K+1}{2}\pm\left\{1+\cos^2 2\phi\left[\left(\frac{K-1}{2}\right)^2-1\right]\right\}^{\frac{1}{2}}. \quad (5)$$

It is seen from Fig. 1 that A_x will be $A\cos\beta$, A_y will be $A\sin\beta$. The tangent of β becomes

$$\tan\beta=\frac{x-\sin^2\phi-K\cos^2\phi}{\sin^2\phi}, \quad (6)$$

where $\beta_2=\beta_1+\frac{1}{2}\pi$. The tangent of β_1 corresponds to the positive sign before the radical in Eq. (5); tan β_2 corresponds to the negative sign before the radical.

Substituting in Eq. (1) for

$$\tau_0^2=\tau_m^2/\cos^2(\theta_B+\phi-\chi)$$

and setting $Q_j=kT$ (which is justified unless the temperature T is very small compared to the characteristic temperature of the crystal) one gets

$$J=C'\cos^2(\theta_B+\phi-\chi)\sum_j\frac{(\boldsymbol{s}\cdot\boldsymbol{A}_j)^2}{v_j^2},$$

where C' may be treated as a constant for given $\boldsymbol{B}_H$, λ and Δ. The summation is now composed of two terms only because of $A_3=k$.

$$(\boldsymbol{s}\cdot\boldsymbol{A}_j)^2=s\cdot(\boldsymbol{A}_j\cdot\boldsymbol{u})^2$$

where $\boldsymbol{u}$ is along the vector $\boldsymbol{B}_H$. Thus,

$$J=C\cos^2(\theta_B+\phi-\chi)\left[\frac{\sin^2(\beta_1-\chi)}{x_1}+\frac{\sin^2(\beta_2-\chi)}{x_2}\right]$$

or, more conveniently for purposes of calculation

$$J=C\cos^2(\theta_B+\phi-\chi)\times\left[\frac{\sin^2(\beta_1-\chi)}{x_1}+\frac{\cos^2(\beta_1-\chi)}{x_2}\right]. \quad (7)$$

It will be discussed later that an additional factor comes into the intensity expression when the α_1 and α_2 radiations are considered.

Referring again to Fig. 1, it is seen that $\lambda\tau_m=\lambda\tau_0\cos(\theta_B+\phi-\chi)$. This also equals $-\Delta\sin 2\theta_B$ and from the figure

$$2\theta=2\theta_B+\Delta\sin 2\theta_B[\tan\theta_B-\tan(\theta_B+\chi-\phi)].$$

This reduces to the more simple expression

$$2\theta=2\theta_B+\frac{2\Delta}{1+\cot\theta_B\cot(\phi-\chi)}, \quad (8)$$

which gives then the scattering angle 2θ in terms of ϕ and Δ.

EXPERIMENTAL DISCUSSION

The data were obtained with a carefully aligned Bragg spectrometer, nickel filtered Cu $K\alpha$ radiation, and x-ray plates which were covered with a 16-micron thick nickel foil to eliminate air-scattered radiation and thus reduce the background of the photographic plate. The slit system was arranged for a horizontal divergence of the incident beam on the crystal face of 9′ of arc for most of the exposures although 18′ divergence was used in two cases. To avoid corrections for horizontal divergence it is only necessary that the horizontal divergence be small compared to the half-width at half-maximum of the pattern or effect being observed. Even with the 18′ divergence the half-widths measured were still much larger. The vertical divergence must, however, be considered. This will be discussed later.

Because the transformer used had only one kilowatt output and the tube was self-rectified, very long exposure times were necessary. The exposures ranged from 20 hours for small displacements to 100 hours for larger displacements.

In the selection of a crystal to be used for these measurements difficulty was encountered in getting a specimen for which the Bragg reflection of a particular plane would not persist over many minutes of arc. If the surface of a crystal is rough, striated, or contains strains from internal stresses it will be found that even upon turning the crystal many minutes or even a degree away from the Bragg angle of incidence the Bragg reflections of α_1 and α_2 will be present after long exposures. This was overcome by using a freshly, and very smoothly cleaved crystal section of an excellent artificial crystal of KCl. Observations were taken down to $|\Delta|=17'$ without the Bragg radiation being present on long exposures. For observations on the 440 plane a crystal was ground at an angle of 45° to eliminate absorption and to produce a focusing effect. To get rid of the Bragg persistence here it was necessary to polish the 45° face with optical rouge on an optical block and carefully etch the surface with alcohol and water. Because KCl and KBr are very soluble in water excessive etching may make the Bragg persistence worse. Each of the crystals finally used had a half-width at half-maximum of the Bragg reflection of the order of 2 minutes of arc. If the shape of the Bragg reflection follows a simple error function it is to be expected that the reflec-

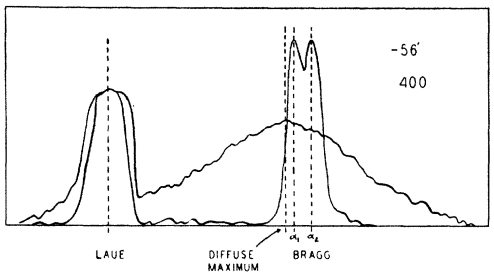

FIG. 2. Photometer tracings of the diffuse maximum for $\Delta = -56'$ with the Bragg $\alpha_1\alpha_2$ super-imposed to demonstrate the displacement of the diffuse from the Bragg angle. The backgrounds which are due to air-scattered radiation have been adjusted to coincide for purposes of comparison.

tion will be completely gone for long exposures at approximately five times its half-width.

A blackening *versus* intensity curve for the $\alpha_1\alpha_2$ radiations was obtained by first taking a series of exposures varying the angle of incidence around the Bragg angle and keeping the time of exposure constant. The resultant curve gave the ratio of the integrated intensity of the $\alpha_1\alpha_2$ sum to the integrated intensity at any crystal setting. Because of the narrow half-width $\alpha_1\alpha_2$ appeared together, fully resolved, however, at only three one-minute interval settings of the crystal. The exposure time was varied for the second curve keeping the crystal fixed at an angle where the intensity of α_1 equaled the intensity α_2. The combination of the two curves gave then the integrated intensity of the $\alpha_1\alpha_2$ combination as a function of the blackening of the photographic plate in terms of the deflections of a microphotometer.

In taking the exposures of the diffuse radiation the following procedure was adopted. The position of the crystal was determined for α_1 intensity equal to α_2 intensity. A short exposure of the order of magnitude of five seconds was made of this Bragg reflection. The crystal was then turned to the selected displacement Δ from the Bragg angle of incidence and an exposure of approximately two hours made to obtain the Laue spot for that particular plane. Another plate was put on the spectrometer without changing the crystal setting or the position of the plate-holder arm and the long exposure for the diffuse radiation made. The first plate thus gave accurately the displacements of α_1 and α_2 from the Laue spot and served as an accurate measurement of the crystal displacement from the Bragg angle of incidence. The second plate gave the displacement of the diffuse radiation from the Laue. The difference, of course, resulted in the displacement of the diffuse line from the $\alpha_1\alpha_2$ positions. The plates were measured by a microphotometer which had a magnification of about 50. Five sets of tracings were taken on the plates to rule out any variations in the microphotometer sensitivity, and to average the shrinkage of the recording paper. The tracings were then reduced to an intensity scale and the displacements, half-widths and intensities measured. Figure 2 is a composite of two photometer tracings. One is the Laue-diffuse plate tracing, the other is the Laue-Bragg plate tracing. The centers of the two Laues are super-imposed as are the backgrounds. The displacement of the maximum of the diffusely scattered radiation

TABLE I. Comparison of theoretical and experimental displacements for various values of delta. (Potassium chloride.) Δ_{α_1} = displacement of crystal from α_1 angle of incidence (29° 18′). δ_{α_1} = displacement of diffuse maximum from the Bragg scattering angle of the α_1 wave-length and is equal to $2\theta_m - 2\theta_{B\alpha_1}$.

HKL	Δ_{α_1} (min.)	Theor. 1* δ_{α_1}	Exper. δ_{α_1}	Theor. 2 δ_{α_1}	Theor. 3 δ_{α_1}
400	−92	− 9.5		−10.3	−44.3
	−56	− 4.75	− 5.0±0.5	− 6.25	−28.0
	−37	− 3.0	− 3.3±0.5	− 4.1	−17.8
	−28	− 2.25	− 2.5±0.5	− 3.1	−13.5
	−17	− 1.5	− 1.0±0.5	− 1.9	− 8.2
	−10	− 1.0		− 1.0	− 4.8
	− 5†	-0.5^{α_1} 8.75^{α_2}		− 0.6	− 1.2
	0†	0.0^{α_1} 9.5^{α_2}		0.0	0.0
	5†	0.5^{α_1} 10.0^{α_2}		0.6	1.2
	10†	1.0^{α_1} 10.5^{α_2}		1.0	4.8
	15†	3.5^{α_1} 10.0^{α_2}		1.7	7.2
	23	8.0	8.0±0.5	2.6	11.1
	31	7.0	6.7±0.5	3.5	14.9
	62	10.5		6.9	29.8
	92	13.5		10.3	44.3
420	−36	− 5.0	−10.0±1.0	−16.0	−21.6
440	−33	−28.0	−25.0±0.5	−30.0	−31.7

* The theoretical results given here under 1 have been calculated from the equations developed in the text with the effect of α_1 and α_2 considered. Column theory 2 has been calculated from the same equations but the mean radiation is used instead of considering the relative effects of α_1 and α_2. Theor. 3 column has been calculated from the less rigorous formula and is inserted here to demonstrate the large difference existing between the two formulae. The equation used here was $2\theta = 2\theta_B + 2\Delta \sin^2 \theta_B$. $\theta_B = 29°22'$.

† At small displacements of the crystal the diffusely scattered radiation will resolve into an α_1 diffuse peak and an α_2 diffuse peak. The superscript indicates the displacement of the α_1 diffuse maximum from the Bragg scattering angle of α_1. The α_2 superscript indicates the displacement of the α_2 diffuse maximum from the Bragg scattering angle of α_1.

from the Bragg scattering angle is well illustrated. The slit divergence in this case was 18′ so the α_1 and α_2 are not well-resolved. The displacements measured on these tracings will be found in Table I.

All probable errors indicated on the drawings or in the tables were calculated by the usual method of taking the square root of the sum of the squares of the individual errors.

THE DISPLACEMENTS OF THE DIFFUSE MAXIMA FROM THE BRAGG ANGLE OF SCATTERING

In analyzing the data obtained it was found necessary to consider the effect of the combination of α_1 and α_2 rather than to take the arithmetical average as is usually done. Thus it is to be seen that the diffuse maximum at, say, $-20'$ will be more strongly affected by the α_1-radiation than $+20'$ will be. In this case of $+20'$ the α_2 will play a more important part.

In making the calculations for the shapes, displacements, and half-widths of the diffuse maxima the equations which resulted from the expansion of the tensor were used. K which was set equal to c_{11}/c_{12} has the value of 6 for KCl. The expression for x (Eq. (5)) was solved by using values of ϕ ranging from $-30°$ to $+90°$. The angle β for each value of ϕ was determined from Eq. (6), and the intensity calculated from Eq. (7). In the case of the 400 reflection χ of course is equal to 0. For the 440 $\chi=45°$, for the 420 $\chi=26°34'$. The factor C for the α_1 radiation is proportional to a factor $2/\Delta^2_{\alpha_1}$, where Δ_{α_1} is the displacement of the crystal from the Bragg angle for α_1. The factor C for α_2 is proportional to $1/\Delta^2_{\alpha_2}$ where Δ_{α_2} is the displacement of the crystal from the Bragg angle for α_2. (The relative intensities of α_1 and α_2 in the incident beam are in the ratio of 2 : 1.) If one considers, then, this additional factor in the computations the intensity of the diffuse line is obtained as a function of ϕ. This is then reduced to a function of 2θ by means of Eq. (8), where $\theta_B=\theta_{\alpha_1}$ or θ_{α_2}, depending on the line radiation being considered. These calculations result in a theoretical diffuse radiation curve for a particular value of Δ considered for either α_1- or α_2-radiation. The analogous curve is then calculated for the other component of the α-radiation and the two curves are combined by adding ordinates. The final curve will then be the theoretical diffuse radiation curve for particular values of Δ_{α_1} and Δ_{α_2}, the difference in the two deltas being, of course, the separation of α_1 and α_2 glancing angles, and for the 400 equal to 5′. From this curve the position and intensity of the maximum is found and the half-width at half-maximum is measured. Each value of Δ is treated in the same manner. Figure 3 demonstrates the displacement δ_{α_1} of the combined diffuse maxima

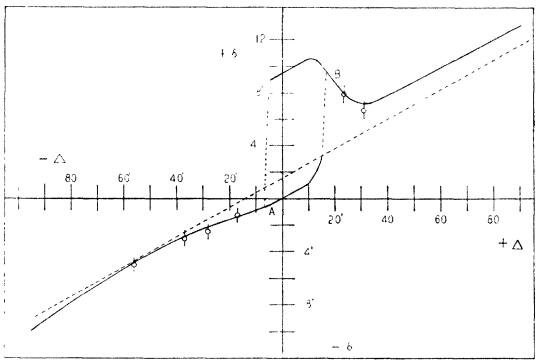

FIG. 3. Theoretical displacement curve for the temperature diffuse maxima. Δ is the displacement of the crystal from the Bragg angle of α_1. δ is the displacement of the diffuse scattering angle from the Bragg scattering angle of α_1. The experimental points with the probable errors are indicated.

from the Bragg scattering angle of α_1. The choice of α_1 as a reference point is purely arbitrary. The displacement δ_{α_2} of the combined diffuse maximum from the Bragg scattering angle of α_2 would be $-10'+\delta_{\alpha_1}$.

In the region of the point A indicated on the drawing the diffuse radiation begins to resolve into an α_1 diffuse maximum and an α_2 diffuse maximum. This condition will exist until at the region of the point B on the + side the effect of the α_2 is small enough to keep the two diffuse maxima from resolving. At the minimum portion of the curves the effect of α_1 is becoming much larger than α_2 and the curve approaches a straight line. The dotted line indicates roughly the effect of the mean radiation on the displacement of the resultant diffuse maximum. If the displacement from the α_1 scattering angle is measured relative to the average Bragg scattering angle (58°44′) the theory predicts a line running through the origin parallel to the dotted

line. Table I gives the numerical values of the experimental results, the theoretical values calculated considering the two component radiations separately, the theoretical values calculated by considering only the mean radiation, and the theoretical values calculated by the less exact formula to be found in an earlier publication.[8]

Also included in Table I are values for the 420 and 440 planes. As has been previously

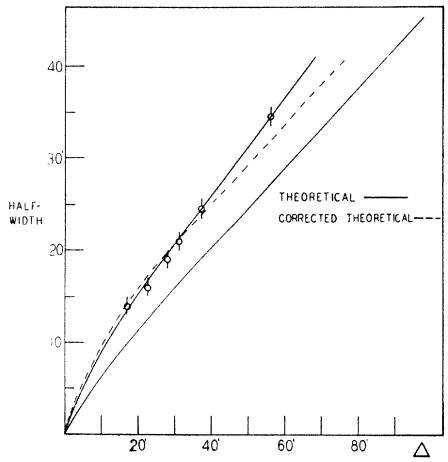

FIG. 4. Half-widths of the diffuse maxima *versus* Δ, the displacement of the crystal from the Bragg angle of α_1. The dotted line represents the correction to the theoretical curve to account for slit divergence.

mentioned the crystal was ground at an angle of 45° to reflect the 440. This procedure eliminated absorption and produced a focusing effect. In the case of the 420 this was not done. The effect of reflecting from an internal plane was to produce large divergence of the reflected beam, this producing, in turn, the same results as if the slits had been very wide. Consequently, the measurements on the 420 are not comparable in accuracy to the 400 and 440. The diffuse radiation of the 420 extended well into the Laue spot which would further destroy the accuracy of the measurements.

THE HALF-WIDTHS OF THE TEMPERATURE DIFFUSE RADIATION MAXIMA

The manner in which the theoretical diffuse maxima curves have been obtained was explained in the preceding section. The theoretical half-widths at half-maxima are measured directly from these curves. Table II gives the numerical values of the experimental and theoretical values and also the corrected theoretical values. Figure 4 demonstrates the relation between these values.

If a' = the theoretical half-width obtained from the theoretical diffuse maximum curve and z = the factors upon which the intensity near a maximum depends, it can be shown that[13]

$$\frac{\frac{1}{2}\tan^{-1}(\phi/a')}{a'} = \frac{\tan^{-1}[\phi/(a'^2+z^2)^{\frac{1}{2}}]}{(a'^2+z^2)^{\frac{1}{2}}}$$

and if $y=z/a'$, $\phi/a=k'$

$$\frac{1}{2}\tan^{-1}(k') = \frac{\tan^{-1}[k'/(1+y^2)^{\frac{1}{2}}]}{(1+y^2)^{\frac{1}{2}}},$$

where ϕ is the vertical divergence of the slit and $=l/2R$. l = height of the slit and R is the distance of the plate from the crystal. In this case $\phi=58'$. By solving this for various values of a', y is obtained equal to a constant multiplied by a'. For a' equal to 10′ the correction factor y becomes 1.5, for a' equal to 20′ y equals 1.35, for a' equal to 40′ y is 1.2. These values are applied to the theoretical curve and the resultant corrected curve is shown in the drawing by the broken line.

It has been reported[10] that the observed half-widths for KCl agreed with the theoretical half-widths as calculated by the less rigorous expression which has been mentioned before. The values which the more exact formula requires are

TABLE II. Comparison of theoretical* and experimental values of the half-widths of the diffuse radiation. (Potassium chloride.)

HKL	$\Delta\alpha_1$ (min.)	Theoretical half-width (minutes)	Theoretical half-width (corrected)	Experimental half-width
400	92	43.5		
	62	28.5	33.5	
	56	27.0	31.0	34.5±1.0
	37	19.0	23.0	24.5±1.0
	31	15.8	19.7	21.0±1.0
	28	15.0	19.0	19.0±1.0
	23	12.5	16.5	16.0±1.0
	17	10.0	13.7	14.0±1.0
420	36	45.0	55.0	50.0±2.0
440	33	20.0	25.0	25.5±1.0

* The theoretical values were corrected by the method described in the text. The effect of the vertical slit divergence is demonstrated in Fig. 4.

[13] S. Siegel and W. H. Zachariasen, Phys. Rev. **57**, 795 (1940).

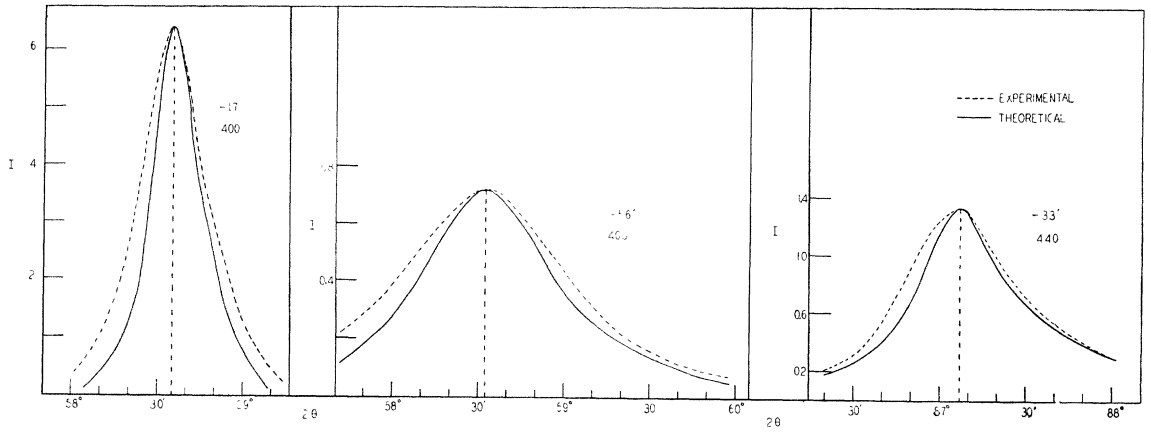

FIG. 5. Experimental and theoretical shapes of the temperature diffuse maxima for three values of Δ.

much smaller than the ones reported in this paper. This discrepancy may be explained by the fact that the plates which the investigator took were rather heavily fogged by air-scattered radiation and consequently, this scattered radiation superimposed upon the diffuse radiation gave half-widths too wide. Another explanation might be that the reduction curve of blackening *versus* intensity was not correct. In any event it is probably safe to assume that the experimental values found by the first mentioned investigator may not be correct.

Figure 5 illustrates the differences in the shapes of the theoretical and experimental diffuse maxima curves. These curves are not corrected for vertical divergence of the slit. The maxima have been adjusted to coincide by means of a constant factor and this factor then applied to the ordinates of the entire experimental curve. For $\Delta_{\alpha_1} = -17'$ it may be noticed that an asymmetry in the curve exists on the right side of the maximum. This is the effect of the α_2-radiation and would be more pronounced if Δ were smaller.

It should be mentioned here that the values for the half-widths are slightly different for + and − values of Δ because of the effect of the two radiations. The differences being so small it was thought unnecessary to include them on the curve.

THE RELATIVE INTENSITIES OF THE DIFFUSE MAXIMA

In any intensity measurement it is the absolute intensity of the effect which is most desired rather than the relative intensities. Because photographic methods in x-ray analyses do not lend themselves to absolute measurements the relative intensity measurements of the diffuse intensity are not to be given great weight in interpreting the phenomena. For this reason no especial care was taken to keep the x-ray tube factors entirely constant over the entire exposure time, particularly in view of the length of exposure. To obtain the experimental relative intensities of the diffuse maxima the maxima were reduced from the blackening to the intensity scale and this divided by the time of exposure. The intensities were then on a relative scale. The theoretical and experimental values were made to agree for $\Delta = -28'$ and the same reduction factor used in reducing the other experimental values. Figure 6 demonstrates the theoretical curve with the experimental points indicated in the usual manner. The dotted line again indicates the theoretical curve corrected for the vertical divergence. Here the corrected intensity will be proportional to

$$\frac{\tan^{-1}(\phi/\Delta \sin 2\theta)}{\Delta}.$$

The corrected theoretical curve is joined to the theoretical curve in the region of $\Delta = 10'$. It is seen that the effect of the vertical divergence is to cause the intensity to approach zero more slowly.

Table III contains the theoretical and experimental relative intensities. The differences in the

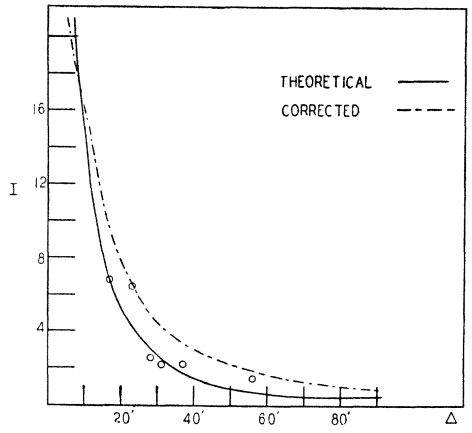

FIG. 6. Theoretical curve for the intensities of the diffuse maxima as a function of Δ. Experimental points indicated by circles.

intensities for + and − values of Δ have been observed but because they are rather small have not been included in the curve, the average being taken instead.

The ratio of the intensity of the temperature diffuse maximum to the integrated intensity of the sum of α_1 and α_2 is found to be of the order of 5×10^{-5} for $\Delta=20'$.

DETERMINATION OF ELASTIC CONSTANTS FROM DIFFUSE SCATTERING DATA

If the present theory concerning the diffuse scattering of x-rays is correct within the limitations it imposes upon itself, namely, that only the forces of the nearest and next nearest neighboring atoms are considered and not the electrostatic forces or the forces due to all the atoms, then from this theory it should be possible to obtain directly the elastic constants of cubic crystals. With enlargement upon the theory to include all symmetry types it should be possible to obtain the elastic constants of crystals having symmetry lower than the cubic arrangement.

With this in mind, diffuse scattering data were obtained for KBr for $\Delta_{\alpha_1}=-35'$ and $\Delta_{\alpha_1}=-17'$. Positive values of the displacement were not considered because of the behavior of the displacement curve in regions close to the Bragg angle.

The experimental results were:

$\Delta_{\alpha_1}=-35'$ $\delta_{\alpha_1}=-6'\pm0.5'$ Half-width $=18'$.
$\Delta_{\alpha_1}=-18'$ $\delta_{\alpha_1}=-5'\pm0.5'$ Half-width $=11'$.

If the diffuse maximum were due to one wavelength instead of two whose relative effects vary with changing Δ, it would be possible to obtain ϕ directly from Eq. (8) for the half-width at half-maximum and for the maximum. Having, then, these two values of ϕ which would correspond to J and $J/2$, it would be possible to solve rather conveniently by trial for the value of $K=c_{11}/c_{12}$ which would satisfy the experimental data. This not being the case because of the two line radiations α_1 and α_2, various values of K were selected and for each value the diffuse maxima plotted for α_1 and α_2 and combined as described before. This was done for $\Delta_{\alpha_1}=-35'$ and $\Delta_{\alpha_1}=-18'$. For $K=3$ the following theoretical values were obtained.

$\Delta_{\alpha_1}=-35'$ $\delta_{\alpha_1}=-7'$ Half-width $=23.5'$,
$\Delta_{\alpha_1}=-18'$ $\delta_{\alpha_1}=-4'$ Half-width $=13'.0$.

The agreement here is not very good, but appears to be the best trial solution. It may only be said then that from preliminary measurements with the method of diffuse scattering the ratio of the constant c_{11} of KBr to c_{12} is very close to 3. $c_{11}=3c_{12}$ is the ideal isotropic case for a cubic crystal, and here x_1, which equals $v_1^2m_a/Vc_{12}$ will equal 3, $x_2=1$, $x_3=1$. The three waves of propagation in the crystal will then be one longitudinal and two transverse. It would seem then, that if $c_{11}/c_{12}\approx3$ for KBr as the diffuse

TABLE III. Comparison of the theoretical and experimental values* of the relative intensities of the diffuse maxima.

HKL	Δ_{α_1} (min.)	Theoretical J/constant	Theoretical (corrected)	Experimental
400	10	16.0	16.3	
	17	6.4	8.9	6.8
	23	4.4	6.2	6.4
	28	2.6	4.8	2.5
	31	2.5	4.2	2.2
	37	1.5	3.3	2.2
	56	0.7	1.8	1.4
	62	0.65	1.5	
	92	0.3	0.8	
440	33	2.9	3.6	3.0

* The experimental values for the intensities were all corrected by the factor which was needed to reduce the experimental value for $\Delta=-28'$ to the uncorrected theoretical value. The theoretical corrected column was calculated by the method discussed in the text which takes into account the vertical divergence of the slits. The theoretical corrected curve and the theoretical curve were joined in the region of 10'.

scattering data would indicate KBr would be a very good substance for using in further investigations. If a monochromatized beam of x-rays were used the complicating factor due to the $\alpha_1\alpha_2$ radiations would be eliminated, at the expense of the intensity of the incident beam, however.

ACKNOWLEDGMENT

The author wishes to thank Professor William H. Zachariasen for his valuable aid and criticism throughout this investigation. We also wish to thank Mr. Paul C. Weyrich of the University of Michigan for the gift of the excellent artificial potassium chloride crystals.

FEBRUARY 1 AND 15, 1942 PHYSICAL REVIEW VOLUME 61

First Spark Spectrum of Neodymium—Preliminary Classification and Zeeman Effect Data

WALTER E. ALBERTSON, GEORGE R. HARRISON, AND J. RAND MCNALLY, JR.
George Eastman Research Laboratories of Physics, Massachusetts Institute of Technology, Cambridge, Massachusetts

(Received November 29, 1941)

Classification by means of the combination principle of 367 lines of Nd II as arising from 30 lower and 57 upper levels has been checked by Zeeman effect measurements at fields up to 87,180 oersteds, and by other data from the M.I.T.-W.P.A. wave-length project. Quantum numbers have been assigned to those levels which have approximate *LS* coupling, and *g* values of all known levels have been determined. The lowest term is $4f^4(^5I)6s-a^6I$. All of the low terms found arise from $4f^46s$ and $4f^45d$, while all identified upper terms are believed to arise from $4f^46p$. The strongest lines in the spectrum belong to the sextet and quartet supermultiplets arising from the transition $4f^4(^5I)6p-6s$, but these show perturbations which give rise to important intensity anomalies which affect the selection of *raies ultimes*. Curves are given which show the variation, in the progression La II, Ce II, Pr II, and Nd II, of the binding of terms arising from the configurations f^ns, f^np, f^nd and, where known, f^{n+1}.

NEODYMIUM ($Z=60$) is third in order of the 14 elements in the Periodic Table called the "rare earths." It gives rise to extremely complex spectra, the normal atom being characterized, according to the Bohr-Stoner theory, by six outer electrons of which several are *f* electrons. No previous known attempt at classification of any of the Nd spectra has met with success, and only by making extensive Zeeman effect studies at high magnetic fields, and by using new determinations of the wave-lengths of lines between 2000 and 11,000A from the neodymium arc, have we succeeded in determining the basic regularities in Nd II.

Some 2700 intense lines of neodymium are listed in the *M.I.T. Wavelength Tables*,[1] while the M.I.T.-W.P.A. card catalog contains a total of 6000 lines believed to arise from this element. Most of these lines can readily be ascribed to the normal atom or the first or second stages of ionization, on the basis of King's[2] studies with the electric furnace. In the present paper 367 Nd II lines are classified as arising from 30 lower and 57 upper levels, to the majority of which quantum numbers have been assigned. Zeeman effect data are included for such of the lines as show resolvable patterns at fields up to 87,180 oersteds. These data suffice to determine the Landé splitting-factors (*g* values) of all terms.

The only Zeeman determinations on Nd lines which we were able to find in the literature were those of Van de Vliet,[3] who reported the separations of a large number of unresolved triplets and resolved patterns for 16 Nd II lines. Van de Vliet used magnetic fields of 38,500 oersteds. Since we had available fields more than twice as strong in

[1] *M.I.T. Wavelength Tables* (John Wiley & Sons, New York, 1939).

[2] A. S. King, Astrophys. J. **78**, 9 (1933).

[3] H. J. Van de Vliet, Thesis Amsterdam (1939).